Nikitina *et al. J Cancer Metastasis Treat* 2023;9:40
DOI: 10.20517/2394-4722.2023.119

Journal of Cancer Metastasis and Treatment

Original Article

Open Access

Check for updates

The contribution of proteoglycans to heterogeneity and temozolomide resistance of glioblastoma cells

Sofia A. Nikitina[1], Dmitry K. Sokolov[1], Alexandra Y. Tsidulko[1], Anastasia V. Strokotova[1], Elizaveta Fasler-Kan[2], Elvira V. Grigorieva[1]

[1]Institute of Molecular Biology and Biophysics, FederalResearchCenter of Fundamental and Translational Medicine (FRC FTM), Novosibirsk 630117, Russia.
[2]Department of Pediatric Surgery Children's Hospital, InselspitalBern, University of Bern, Bern 3010, Switzerland.

Correspondence to: Dr. Elvira V. Grigorieva, Institute of Molecular Biology and Biophysics, Federal Research Center of Fundamental and Translational Medicine (FRC FTM), Timakova str. 2, Novosibirsk 630117, Russia. E-mail: elv_grig@yahoo.com

How to cite this article: Nikitina SA, Sokolov DK, Tsidulko AY, Strokotova AV, Fasler-Kan E, Grigorieva EV. The contribution of proteoglycans to heterogeneity and temozolomide resistance of glioblastoma cells. *J Cancer Metastasis Treat* 2023;9:40. https://dx.doi.org/10.20517/2394-4722.2023.119

Received: 29 Sep 2023 **First Decision:** 15 Nov 2023 **Revised:** 29 Nov 2023 **Accepted:** 11 Dec 2023 **Published:** 26 Dec 2023

Academic Editor: Ciro Isidoro **Copy Editor:** Fangyuan Liu **Production Editor:** Fangyuan Liu

Abstract

Aim: Heterogeneity of glioblastoma (GB) cells significantly contributes to tumor resistance against temozolomide (TMZ) and the development of disease relapse. Multiple molecular mechanisms are involved in this process, yet the contribution of proteoglycans (PGs) remains unknown. This study aimed to investigate the potential involvement of PGs (both at core proteins and polysaccharide chains) in the heterogeneity and TMZ resistance of GB cells.

Methods: Seven human GB cell lines were characterized for TMZ sensitivity, cell phenotypic traits, gene expression for glucocorticoid receptor (GR, *NR3C1*), PG core proteins- and heparan sulfate (HS) biosynthesis-related genes and content of their chondroitin sulfate (CS) and HS chains.

Results: Although the studied cell lines have similar proliferation rates, they significantly differ in their migration activity, clonogenicity, and TMZ resistance (IC_{50} 8.51-369.59 μM in the line of U343, LN215, HS683, U87, LN71, LN405, LN18), creating a specific phenotype for each cell line. Some PGs (NG2/CSPG4, CSPG5, and versican) contributed to the molecular heterogeneity of these cells being cell line-specifically expressed in all cell lines, which also differed in terms of the CS/HS content. Transcriptional activity of the HS metabolic system was low in these GB cell lines, expressing mainly EXT1/2 and NDST1/2, while expression levels of sulfotransferases and SULF2 were

cell line-specific. TMZ resistance of these cells was correlated with the expression of stem-cell marker CD44 (+3.5-fold, r = 0.73) and GR (-3-fold, r = -0.81). TMZ treatment of the resistant (LN405) and sensitive (LN215) cells resulted in complex changes in cell migration as well as NG2/CSPG4 expression and CS/HS content.

Conclusion: Differential expression of PGs and CS/HS content contribute to the heterogeneity of GB cells, and CD44 and NR3C1 might be informative biomarkers for TMZ resistance.

Keywords: Glioblastoma, temozolomide resistance, extracellular matrix, proteoglycan, glycosaminoglycan, heparan sulfate, chondroitin sulfate, glucocorticoid receptor

INTRODUCTION

Glioblastoma (GB) is characterized by a well-known phenomenon of extremely high structural and functional heterogeneity of GB cells within the same tumor. The heterogeneity is a basis for the clonal selection of cancer cells under the pressure of chemotherapeutic drug(s) and acquiring resistance to the treatment, which contributes to the disease relapse[1]. Heterogeneity usually encompasses both inter-tumor heterogeneity between the individual tumors and intra-tumor heterogeneity between the cells within the same tumor[2]. In GB, although the variability of the different tumors is relatively low, intra-tumor heterogeneity is very high[3]. The variability of cancer cell phenotypes in a GB tumor leads to insufficient effectiveness of anti-GB treatment because, among a heterogeneous population, there are always cells that can resist therapy[4,5]. A possible solution could be the creation of a number of drugs that could be alternated during GB treatment, but unfortunately, the present standard of GB care has remained largely unaltered since 2005[2,6]. This treatment regimen includes TMZ as the first-line systemic treatment, but most patients do not respond to TMZ properly and relapse after 6-9 months[7].

The most commonly accepted reason for this effect is an arising resistance to TMZ[8,9], which develops through multiple molecular mechanisms[10-13]. Among them are both tumor intrinsic factors and tumor microenvironment (TME)-dependent factors[14,15], such as crosstalk between GB and glial cells[16], various immune and non-immune cellular components of TME[17-19] and extracellular components involved in cell-matrix interaction and signaling[20,21,4]. Many approaches to overcoming TMZ resistance in GB cells are currently being proposed, but so far, none of them has come close to real clinical practice[22,23], which supports the need to continue active investigation of molecular mechanisms of TMZ resistance.

A comparative study of different GB cell lines represents a conventional model for the investigation of the heterogeneity of GB cells and their characterization according to various parameters.

The cell motility dynamic was studied in U373 and U87 GB cell lines[24]; seven GBM cell lines (SNB-19, GaMG, U251, U87, U373, U343, U138) were analyzed for the expression of MMP-1, -8-11, -13, -17, -19-21, -23, -24, -26-28[25]; status of TP53, p16, p14ARF, and PTEN tumor suppressor genes was determined for 34 human glioma cell lines[26]; the standard 16 marker short tandem repeat (STR) DNA fingerprints is reported for a panel of 39 widely used glioma cell lines[27]; four human malignant glioma cell lines (LN215, LN235, LN308, LN992) were characterized for karyotype, CNPase activity, myelin, S-100, and GFAP proteins[28]. An interesting U-343 model was used in the study by Guo et al., consisting of a set of distinct GB cell lines derived from the same tumor (U-343 MG, U-343 MGa, U-343 MGa 31L, U-343 MGa Cl2:6)[29]. These cells were characterized with regard to DNA copy number, gene expression profile, protein secretome, TMZ sensitivity, and cancer cell phenotypic traits, and demonstrated distinct gene expression profiles and phenotypes in spite of they were derived from a single tumor.

Among these multiple functional and molecular parameters, studies of the expression and content of glycosylated molecules such as PGs have an important place and increasing data indicate that PGs can also contribute to the heterogeneity of GB cells: the expression of NG2/CSPG4 identifies an aggressive and actively cycling GB cells population[30]; a barcode labeling approach in combination with phenotyping to characterize two cell lines derived from IDH-wild type GB identified a remarkable heterogeneity of the phenotypes between the cell lines including CD44[31]; the expression of CD44 differs between proliferating and non-proliferating glioma cells[32] and correlates with cell proliferation, intra-tumor heterogeneity and phenotype stability[33]. As one can see, most of the publications are related to CD44 due to the known role of this molecule as a stem-cell marker[34], while the role of other PGs and glycosaminoglycans (GAGs) such as chondroitin sulfate (CS) and heparan sulfate (HS) in GB cell heterogeneity remain underinvestigated as well as their involvement in TMZ resistance of GB cells.

In this study, the possible involvement of glycosylated macromolecules (PGs, CS, HS), HS biosynthetic system as well as its potential transcriptional regulator GR (*NR3C1*) in the heterogeneity of GB cells and their resistance to TMZ was investigated in the GB cell lines model *in vitro*.

METHODS

Cells

The human glioma cell lines U87, U343, HS683, LN18, LN71, LN215, and LN405 used in this work were from the ATCC (Manassas, VA, USA). Cell lines were accompanied by authentication certificates and cultured according to the ATCC recommendations. Cell line characterization is presented in Supplementary Table 1.

All cell lines were maintained in IMDM medium with fetal bovine serum/L-glutamine/penicillin/streptomycin supplements at 37 °C in a humidified 5% CO_2 incubator. For analysis, the cells were harvested using trypsin/EDTA and fixed with RNALater (ThermoFisher Scientific, Waltham, MA, USA) according to the manufacturer's instructions.

Treatment of the cells with TMZ (MSD, Finland) was performed for 120 h with daily change of the TMZ-containing medium. After 5 days of incubation, this medium was removed, and the cells were grown up to 90%-95% confluency and collected for analysis.

Temozolomide resistance assay

Cells were seeded at 2,000 cells per well in a 96-well plate. After 48 h, TMZ (MSD, Espoo, Finland) was added to the plate at 16, 32, 63, 125, 250, 500 и 1,000 μM, and the cells were incubated in the 5% CO_2 incubator at 37 °C for 6 days. Every 24 h, Hoechst and propidium iodide were added to some wells, incubated for 30 min and scanned using a high-performance screening system In Cell Analyzer 2200 (Cytiva, Marlborough, MA, USA). Five fields of view in the light field, blue and red channels were photographed, and the amount of total, dead, and apoptotic cells was counted.

Cell proliferation assay

Cell proliferation rate was estimated using the CYQUANT Direct Cell Proliferation Assay (Invitrogen, Waltham, MA, USA) according to the manufacturer's instructions. Briefly, cells were seeded in a 96-well microplate at 2,000 cells per well and the DNA content was measured for 4-6 days every 24 h by adding 50 mL of fluorescent dye followed by incubation at 37 °C for 1 h. The fluorescence intensity was measured at 485/530 nm using a microplate reader WallakEnVision (PerkinElmer, Markham, ON, Canada). The average doubling time of the number of cells was determined by the formula dt × log2/(logN2 - LogN1),

where log is the decimal logarithm, "dt" is the time interval between the measurement points, N1 is the number of cells at the first time point, and N2 is the number of cells at the second point.

Migration assay

Cells were grown in a 12-well plate at high density (≥ 90% confluency), and two scratches were applied crosswise on the cell layer with the tip. The position of the scratches was fixed using a ZOE microscope (Bio-Rad, Hercules, California, USA) and monitored 6 or 24 h after the scratching. Quantification of the images was performed with ImageJ software (Wound healing size tool) and measured as % of the initial scratch area.

RT-PCR analysis

Total RNA was isolated with the RNeasy Plus Mini Kit (Qiagen, Germantown, MD, USA) and its concentration was determined with Qubit RNA BR Assay Kit (ThermoFisher Scientific, Waltham, MA, USA) according to the manufacturers' instructions. 0.5 μg of the RNA was used for the reverse transcription by the RevertAid First Strand cDNA Synthesis kit (Thermo Fisher Scientific, Waltham, MA, USA) and 0.25 μL of the product was used for each PCR amplification. RT-PCR analysis was performed on CFX96™ instrument (Bio-Rad, USA) using the Taq-pol (IMCB, Novosibirsk, Russia) and BioMaster HS-qPCR SYBR Blue master mix (Biolabmix, Novosibirsk, Russia) in 20 μL. PCR conditions were: 95 °C for 5min, then 40 cycles at 95 °C for 10 s, 59 °C for 15s and 72 °C for 30 s. The intensity of the amplified DNA fragments was normalized to that of GAPDH. The fold change for each mRNA was calculated by the $2^{\Delta Ct}$ method. Bars on the graphs represent the mean ± SD from triplicate experiments (OriginPro8.1). Primer sequences for human PG core protein genes are presented in Supplementary Table 2.

Immunofluorescence

For immunofluorescence analysis, cells were grown on glass coverslips, fixed with phosphate-buffered 4% formaldehyde for 10min and permeabilized with 0.1% Triton-X100 in PBS. Non-specific staining was blocked with 1% BSA in PBST for 30 min at room temperature (RT) before the incubation with rabbit polyclonal anti-NG2 (Abcam, Cambridge, UK, ab83178; 1:100), mouse monoclonal anti-HS (Millipore, MAB2040; 1:100) or mouse monoclonal anti-CS (Sigma-Aldrich, Burlington, MA, USA, C8035; 1:100) primary antibodies in 1% BSA in PBST at RTfor 1 h. After rinsing with PBST (3 × 15 min), cells were incubated with anti-mouse Alexa Fluor 488 (Abcam, Cambridge, UK, ab150117; 1:1,000) or anti-rabbit Alexa Fluor 488 (Abcam, Cambridge, UK, ab150063, 1:1,000) secondary antibodies at RTfor 1 h, rinsed with PBST (3 × 10 min). The slides were mounted using SlowFade Diamond Antifade mounting medium with DAPI (ThermoFisher Scientific, Waltham, MA, USA) and imaged on a ZOE microscope (Bio-Rad, Hercules, California, USA). Quantitative analysis of the images was done using ImageJ software.

Cell surface glycosylation

To estimate a GAG content on the cell surface, the cells were treated with 0.05% trypsin in 0.53 mM EDTA and centrifuged at 3,000 rpm. The supernatant (100 μL) was mixed with 500 μL of dimethylene blue (80 μM dimethylene blue, 5% EtOH, 0.2 M GuHCl, 0.2% HCCOH), incubated for 24 h at RT, and centrifuged at 12,000 prm for 10 min. The pellet was dissolved in 125 μL of dissociation solution (4 M GuHCl, 50 mM AcONa) for 10 min with vortexing and measured using spectrophotometer WallacEnVision (PerkinElmer, Markham, ON, Canada) at 656 nm. The calibration curve was created using chondroitin sulfate C (Sigma-Aldrich, Burlington, MA, USA). Normalization was performed on the initial cell count.

Statistical analysis

Statistical analyses were done using the ORIGIN 8.1 program(OriginLab Corporation, Northampton, MA, USA). Data are expressed as means ± SD, and a value of $P < 0.05$ was considered statistically significant.

Pearson correlation coefficients (r) were used to investigate an association between the studied parameters. The statistical significance of the linear correlation coefficient ($P < 0.05$) was estimated using a table of critical values of the Pearson coefficient.

RESULTS

The collection of the used GB cell lines represents an *in vitro* model to investigate molecular mechanisms underlying the chemoresistance of GB cells. It is composed of seven different cell lines, most of them clearly denoted as GB cell lines (LN18, LN71), while for some, there is no clear consensus about their origin [Supplementary Table 1]. Counting this uncertainty and the fact that, in recent years, there has been an active revision of the classification of tumors according to their molecular characteristics[35-39], we decided to use all these cell lines in the study.

Resistance of these cells to TMZ was determined as a TMZ concentration leading to a 2-fold decrease in the proliferation rate of the studied cells (IC_{50}) [Supplementary Table 3]. On the graph, the studied cell lines were arranged in ascending order of resistance to the TMZ effects, demonstrating a difference of up to two orders of magnitude on this parameter [Figure 1A].

It is interesting that cell proliferation rates and doubling times were similar for all cell lines [Figure 1B and C], whereas migration activity [Figure 1D] and content of the cell surface GAGs [Figure 1E] were characteristic for individual cell lines, and collectively created a complex combination of the functional parameters specific for each cell line.

Profiling of the expression of the PG core protein genes showed that CSPGs CD44, biglycan, NG2/CSPG4 [Figure 2A] and HSPGs syndecan-3, glypican-1 [Figure 2B] were the most expressed PGs in the human GB cells [Supplementary Table 4].

In addition, the conditional assign of PGs into CSPGs and HSPGs revealed a tendency for an increase in CSPG expression and a decrease in HSPG expression as the TMZ resistance increased [Figure 2A and B].

A major contribution to the increase in the total CSPG pool was made by the most abundant CSPG CD44 (up to +3.5-fold), known as a biomarker for cancer stem cells. Although the positive correlation of CD44 expression with TMZ IC_{50} ($r = 0.73$) was not very strong, the most TMZ-resistant LN18 cell line possessed the highest CD44 expression level [Figure 2A and C] along with the lowest doubling time [Figure 1C]. The combination of the functional (low proliferation rate, active migration, TMZ resistance) and molecular (high CD44 expression) characteristics of the LN18 cells suggests this cell line is stem-like cells. This may be of importance in the designing of experimental *in vitro* models to study GB cell heterogeneity.

At the same time, CSPG brevican (-2-2.5-fold) [Figure 2C] and HSPG syndecan-1 (-4-5-fold) [Figure 2D] demonstrated an opposite trend, being significantly negatively associated with TMZ resistance of these GB cell lines ($r = -0.85$ and $r = -0.75$, respectively). However, extremely low baseline expression levels of these PGs do not allow us to conclude with certainty about the degree of their real participation in the development of TMZ resistance.

An interesting expression mode was observed for neuro-glial antigen NG2/CSPG4 (biomarker for oligodendrocyte progenitor cells, related to GB resistance to radiotherapy) in different GB cell lines. It was expressed to a different extent in three cell lines (LN215, U87, and LN405), with almost no expression in U343, HS683, LN71, and LN18 cells [Figure 2C].

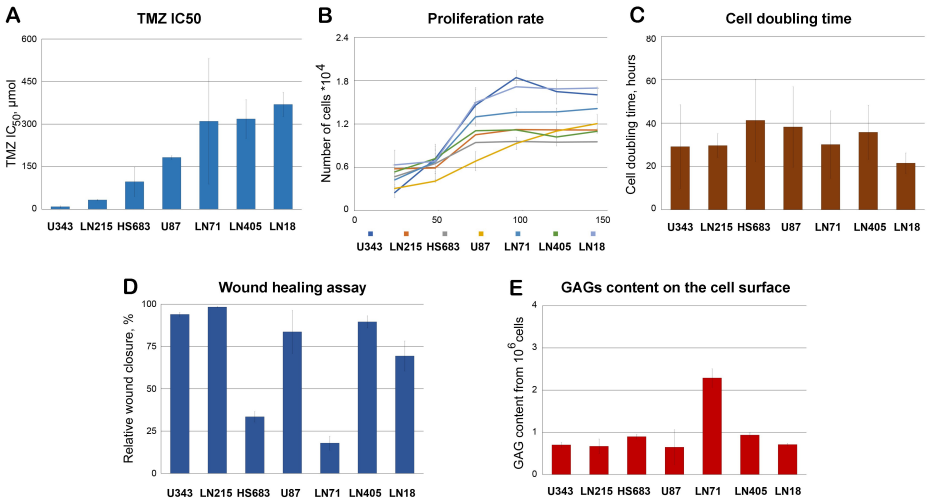

Figure 1. Characterization of human GB cell lines. (A) TMZ resistance of the cells (IC_{50} for TMZ). (B) Proliferation rates (CyQuant Assay). (C) Doubling time. (D) Migration activity (Wound healing assay, wound closure for 24 h). (E) GAGs content on the cell surface. Cell lines are placed in the order for TMZ resistance (A); all other graphs are arranged in the same cell line order.

We performed the immunofluorescence characterization of NG2/CSPG4 expression as well as the content of polysaccharide CS and HS chains in all cell lines [Figure 3].

The obtained data confirmed heterogeneity of the studied cell lines in terms of NG2/CSPG4 expression at the protein level and showed heterogeneity in CS and HS content as well.

It is interesting that the overall transcriptional activity of the genes involved in the HS biosynthetic machinery did not demonstrate significant heterogeneity in these cell lines except TMZ-sensitive LN215 cells and the most TMZ-resistant LN18 cells [Figure 4].

Such increased expression of HS metabolism-involved genes in LN215 and LN18 cells was mainly due to the elevated expression of EXT1/EXT2 responsible for the elongation of the growing HS chain during biosynthesis. At the same time, expression of the genes of post-synthetic HS modification demonstrated similar levels in all cell lines, and the highest heterogeneity was observed for genes responsible for HS sulfation (HS6ST2) and desulfation (SULF2) (unlike HS3ST1/2 and SULF1 not presented on the figure) [Figure 4B].

Most of the studied PG biosynthesis-involved genes have a glucocorticoid-responsive element in their promoter, and we hypothesized that GR (Nuclear receptor subfamily 3 group C member 1, *NR3C1*) might be associated with the gene expression levels. To check for possible involvement of GR in the transcriptional regulation of HS metabolism-involved genes, we investigated the GR expression in the GB cell lines and its correlation with the TMZ resistance of these cells [Figure 5].

Surprisingly, there was a correlation of GR expression with TMZ resistance of the GB cells (r = -0.81) [Figure 5B] but not the expression level of HS biosynthesis-involved genes, and this result warrants further investigation.

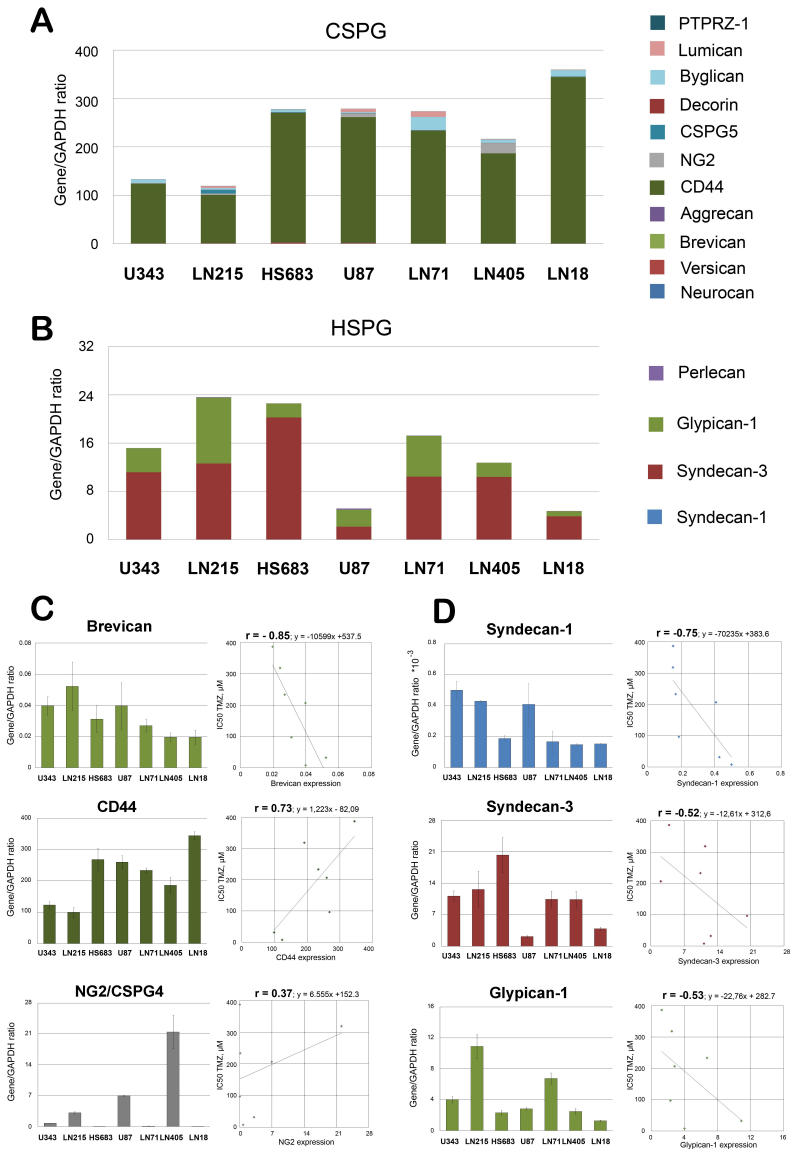

Figure 2. Expression of PG core proteins in human GB cell lines. (A and B) Expression pattern of the CSPG (A) and HSPG (B) core protein-coding genes. The stacked columns reflect the contribution of each gene to the total expression level. (C and D) Individual CSPG (C) and HSPG (D) genes. RT-PCR analysis. Right panels - correlation analysis between the expression level and TMZ resistance for each individual gene. r - Pearson correlation coefficient. (A-D) Cell lines are placed in the order for TMZ resistance.

Taken together, the obtained data shows that GB cell lines differ by both the pattern and the expression levels of GR, by some PGs (CD44, brevican, NG2/CSPG4, syndecan-1, syndecan-3, glypican-1) and by the content of their polysaccharide GAG chains (CS, HS). A specific combination of the expressed PG and CS/HS content creates a unique phenotype of each GB cell line, and the presence or absence of CSPG CD44 and GR correlates with TMZ resistance of these cells, suggesting these molecules as potential biomarkers of TMZ resistance.

An interesting question was whether TMZ treatment has any effect on the functional parameters of the GB cells that we have studied. For that, the most sensitive (LN215) or resistant (LN405) GB cells were treated with TMZ and their phenotype was investigated [Figure 6].

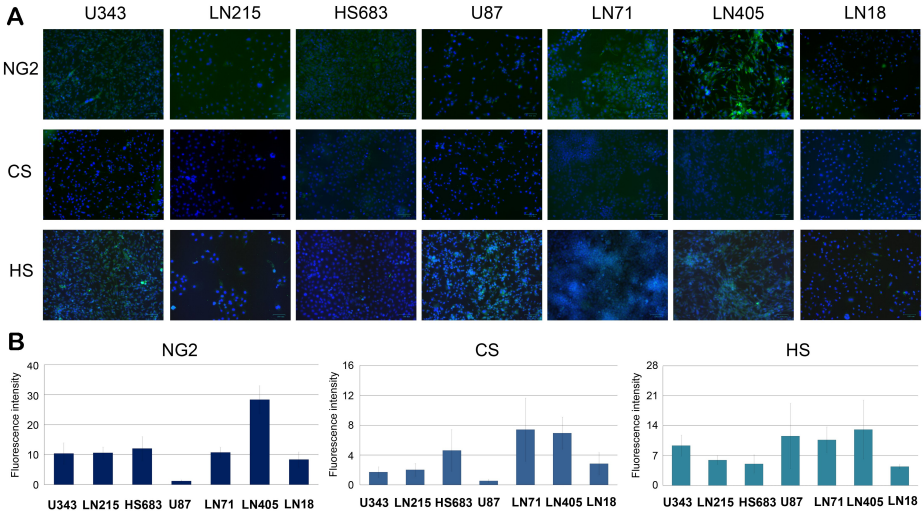

Figure 3. Immunofluorescence analysis for NG2/CSPG4 core protein and CS and HS content in human GB cell lines. (A) Representative microphotographs of immunostaining with anti-NG2, anti-CS, and anti-HS antibodies (Alexa Fluor 488). Magnification ×200, the scale bar for the micrographs is 100 µm. (B) Quantification of the NG2/CSPG4 protein, CS and HS content in the cells -average fluorescence intensity calculated using MeanGrayValue (ImageJ). ANOVA + Fisher's LSD test. CS: chondroitin sulfate; HS: heparan sulfate.

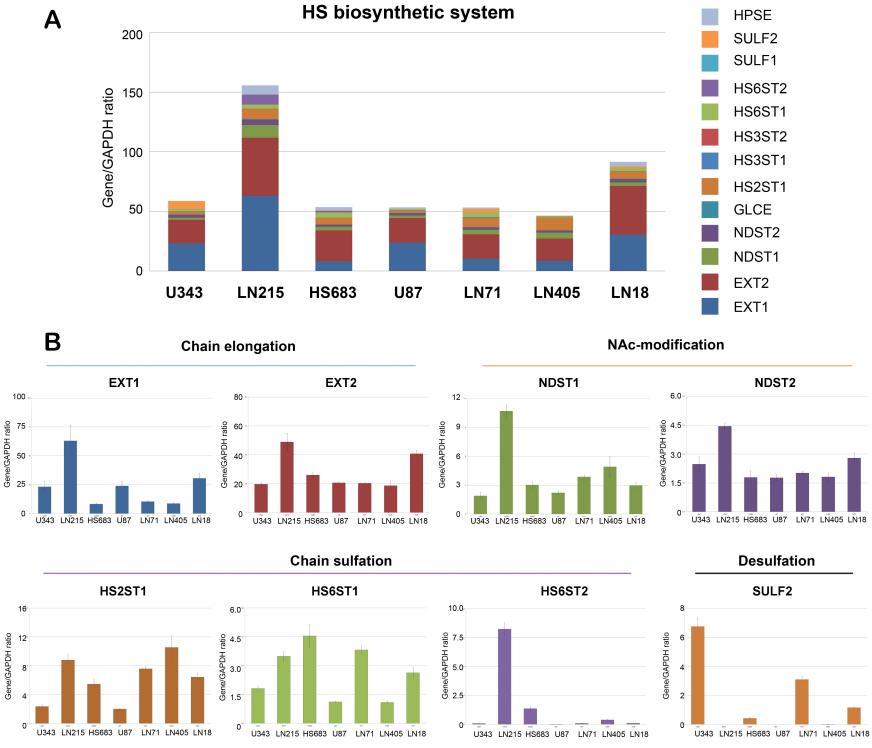

Figure 4. Transcriptional activity of the HS metabolic system in human GB cell lines. (A) Overall transcriptional activity of HS metabolism-involved genes. The stacked columns reflect the contribution of each gene to the total expression level. (B) Expression of the individual genes, showing significant variability of the expression level in the studied cell lines. (A and B) Cell lines are placed in the order for TMZ resistance.

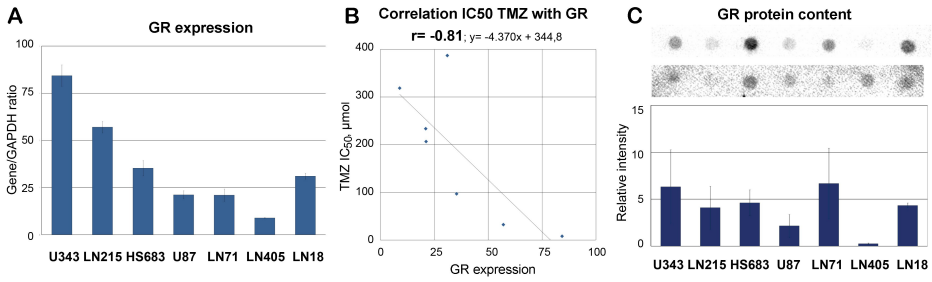

Figure 5. GR expression in human GB cell lines. (A) Expression of GR at mRNA level. (B) Correlation analysis for the GR expression levels and TMZ resistance. r - Pearson correlation coefficient. Cell lines are placed in the order for TMZ resistance. (C) GR protein content in the GB cells (dot-blot analysis with anti-GR primary antibody).

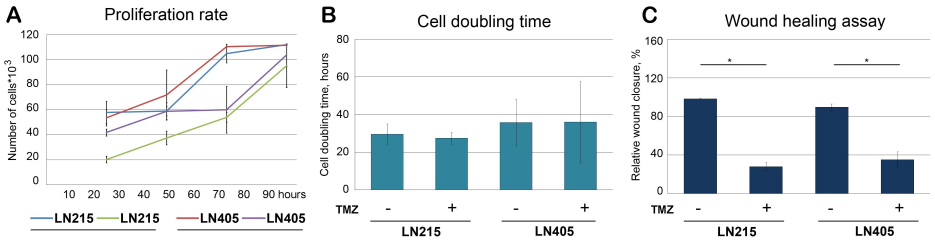

Figure 6. Effects of TMZ on the phenotypic traits of the studied GB cell lines. (A) Proliferation rates (CyQuant Assay). (B) Doubling time. (C) Migration activity (Wound healing assay, wound closure for 24 h) of the studied GB cells. Cell lines are placed in the order for TMZ resistance. * $P < 0.05$.

TMZ treatment did not affect the proliferation rates of both cell lines [Figure 6A and B], but it significantly decreased their migration potential [Figure 6C].

As for PGs, the TMZ-resistant LN405 cells responded to TMZ by a decrease in NG2/CSPG4 expression (at the mRNA and protein levels) [Figure 7A-D], whereas TMZ-sensitive LN215 cells demonstrated main changes in the GAG content, such as an increase in CS content (+2.5-3-fold) and a decrease in HS content (-1.5-2-fold) [Figure 7C and D].

Interestingly, TMZ treatment had the opposite effect on the expression of CD44 in different GB cell lines. In the TMZ-resistant LN405 cells, TMZ decreased the CD44 expression level, whereas the similar treatment of the TMZ-sensitive LN215 cells increased the CD44 expression level in these cells [Figure 7A], shifting them (on this parameter) to a more stem cell-like molecular pattern.

These changes in GAG content indicate that under TMZ pressure, the phenotype of TMZ-sensitive LN215 cells becomes more similar to the phenotype of TMZ-resistant cells, which could be a new molecular mechanism for the development of TMZ resistance in GB cells. Thus, the changes in the content of glycosylated molecules in GB cells during chemotherapy might reflect the development of TMZ resistance.

DISCUSSION

Despite the active adjuvant radiochemotherapy, many GB patients do not respond to TMZ during the course of their treatment[8,11], and the identification of molecular markers of the drug resistance remains a current challenge. Such biomarkers can be used to predict patient survival or even as targets for the development of new approaches to overcome drug resistance and prolong patients' survival[40]. In this study,

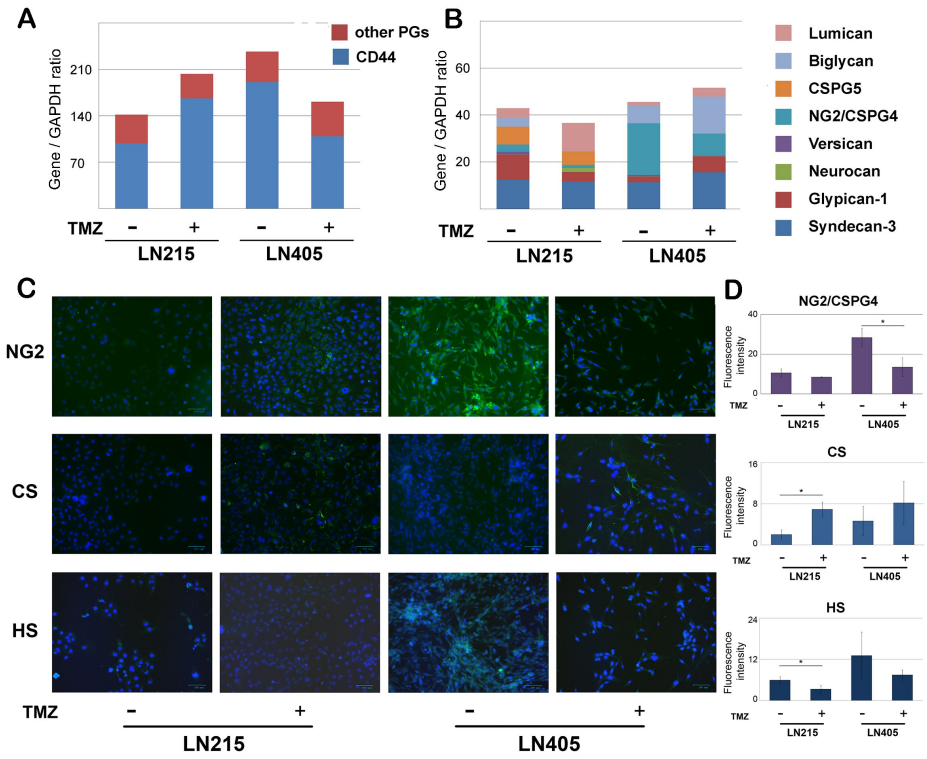

Figure 7. TMZ effects on the PGs expression and GAG content in the GB cell lines. (A and B) Expression of PG core proteins - CD44 and others (A) and all PGs except CD44 (B). RT-PCR analysis. (C) Immunofluorescence analysis for NG2/CSPG4 core protein and CS and HS content. Representative microphotographs of immunostaining with anti-NG2/CSPG4, anti-CS, and anti-HS antibodies (AlexaFluor 488). Magnification ×200, the scale bar for the micrographs is 100 µm. (D) Quantitative analysis - average fluorescence intensity calculated using MeanGrayValue (ImageJ). ANOVA + Fisher's LSD test. CS: chondroitin sulfate; HS: heparan sulfate. * $P < 0.05$.

we showed that PGs contribute to the molecular heterogeneity of GB cells being ubiquitously (CD44, syndecan-3, glypican-1, biglican, brevican) or cell line-specifically (NG2/CSPG4, CSPG5 and versican) expressed in all studied GB cell lines, with a common tendency to an increased CSPG and decreased HSPG expression in TMZ-resistant cell lines (LN405, LN18). These results stay in line with few data on the important functional role of some PGs in GB development. It was recently shown that glypican-1-silenced U-251 MG cells were much more sensitive to TMZ than an intact cell line[41]; CD44 is associated with stemness of GB cells and its knock-out deregulates the expression of the genes related to the hyaluronan synthesis and degradation, interacting matrix proteins and PDGF isoforms and PDGF receptors[42]; high CD44 expression was furthermore correlated with poor prognosis of GB[43]. Surprisingly, TMZ resistance of the studied GB cells was associated with the expression level of CSPG CD44, which is widely known as a stem-cell biomarker including GB ($r = 0.73$).

In addition to the specific expression of PG core proteins, the studied GB cell lines showed significant heterogeneity (2-3 times) in the content of carbohydrate chains of CS and HS. These results stay in line with the data by Tran et al. about the heterogeneity of HS disaccharide content and structure in primary GB tumorsphere lines obtained from individual human or murine GB tumors[44]. Together, these data extend our knowledge of the important role of HS in brain carcinogenesis[45]. As to CS content, its significant variability in the different GB cell lines does not correlate with TMZ resistance of these cells, although it can be meaningful in terms of some other (unknown yet) molecular or functional characteristics of GB tumors.

Indirect evidence in favor of such a hypothesis is supported by the data of Jaime-Ramirez *et al.*, who showed that Chondroitinase (Chase) ABC (an enzyme that cleaves CS polysaccharide chains from CSPGs in the tumor ECM) significantly increases the toxic effects of TMZ, and intratumoral administration of a ChaseM-TMZ combination results in significant enhancement in survival compared to each individual treatment alone[46]. Overall, the obtained results on the evident contribution of glycosylated extracellular macromolecules (PGs, CS, HS) to GB cell heterogeneity warrant further investigation.

Interestingly, TMZ treatment significantly affects the molecular and functional characteristics of the studied GB cells, and these changes differ for TMZ-resistant and TMZ-sensitive cells. For TMZ-resistant LN405 cells, TMZ decreases the expression of NG2/CSPG4 protein shown as a marker of chemo- and radio-resistance of cancer cells, whereas for TMZ-sensitive LN215 cells, it decreases HS content and increases CS content [Figure 7]. Such TMZ-induced changes suppose a deterioration of PG/GAG composition in the GB cells, contributing to their shift to more or less aggressive phenotype. These data complement our previous results on the significant effects of TMZ on PG/GSG expression and composition in normal brain tissue in the animal models of GB relapse[47]. The TMZ-treated rat and mouse brain tissue was more susceptible to U87 GB cells, providing favorable conditions for the development of U87 xenografts in SCID mice[48]. Together, these results show that TMZ treatment affects PGs/GAGs in both GB cells and surrounding normal brain tissue and can take part in the mutual adaptation of the cancer cells with their microenvironment.

Transcriptional profiling of the genes involved in HS biosynthesis revealed an interesting effect related to the relative stability of the transcriptional activity of enzymes responsible for HS chain elongation (EXT1, EXT2), and GB cell line-specific expression of sulfotransferases HS2ST1, HS6ST1/2, and SULF2. This probably indicates that TMZ resistance can be related to the different sulfation of HS chains in phenotypically different GB cells. Similar heterogeneity in the expression of some individual HS metabolism-involved genes (SULF2, HPSE) was shown in the primary tumorspheres from the human and mouse GB tumors, where some of them demonstrated high expression levels of SULF2 and others that for HPSE[44]. These few data on the involvement of HS and HS metabolic machinery in the heterogeneity and phenotype of GB cells warrant further research in this direction.

Keeping in mind that the HS biosynthetic system might be regulated or coordinated by transcription factor NR3C1 (GR), we determined its expression in all studied cell lines, expecting a possible correlation of these parameters. However, the GR expression in the studied GB cancer cells was not associated with the expression levels of HS biosynthesis-involved genes, and this result fits well with our previously published data on the correlation of GR with these genes in normal brain tissue and U87 xenografts. It was shown that normal brain tissue is characterized by a high correlation of GR expression with most of the genes involved in the biosynthesis of PG (20 of 28 genes had a correlation coefficient with the level of GR $P = 0.81\text{-}0.97$, $P < 0.05$). However, the introduction of dexamethasone (DXM) led to the dose-dependent disappearance of this correlation, which was intensified over time, almost completely disappearing by 7-10 days after DXM administration[49]. At the same time, the xenograft U87 tumors grown in the intact SCID mouse brain did not demonstrate such correlation, although it was present in the U87 xerographs grown in the TMZ and/or DXM pre-treated animals where a significant positive correlation between the expression of GRalpha (but not GRbeta) isoform with a number of HS metabolism-involved genes (such as Ext1/2, Ndst1/2, Glce, Hs2st1 and Hs6st1/2) was observed[50]. Taken together, these results suggest deterioration of transcriptional regulation of the HS biosynthetic system by GR in GB cancer cells, which can be partially reverted upon the treatment of these cells/experimental tumors with TMZ/DXM.

Another interesting result is a significant association of GR expression in GB cells with TMZ resistance of these cells (r = -0.81), suggesting GR for the first time as a potential player in TMZ resistance development. To date, there are no published results for comparison.

Considering these results together, a set of two molecular markers of TMZ resistance - GR and CD44 - might be suggested. An important moment is that these molecules have opposite changes in TMZ-resistant cells, representing qualitative changes in the tested GB tumors, as opposed to the quantitative approach, where a robust control is necessary to determine the expression of each of these genes. The presence of GB cells with simultaneously increased expression of CD44 and decreased expression of NR3C1 might be informative biomarkers for TMZ resistance.

DECLARATIONS

Acknowledgments

The authors thank the Center for Collective Use "Proteomic Analysis" (organised by the Ministry of Science and Higher Education of the Russian Federation, agreement No. 075-15-2021-691) for the provided equipment. A.V.S. is very grateful to the Russian Federation President Scholarship Program for young scientists (SP-4000.2022.4).

Authors' contributions

Made substantial contributions to the conception and design of the study and performed data analysis and interpretation: Tsidulko AY, Fasler-Kan E, Grigorieva EV
Performed data acquisition and interpretation: Nikitina SA, Strokotova AV, Sokolov DK, Grigorieva EV
Provided administrative, technical, and material support: Fasler-Kan E, Grigorieva EV
Writing and editing: Sokolov DK, Strokotova AV, Fasler-Kan E, Grigorieva EV

Availability of data and materials

The original data presented in the study are included in the article. Further inquiries can be directed to the corresponding author.

Financial support and sponsorship

This work was supported by the Russian Science Foundation (Grant No. 21-15-00285) in part of GR and HS biosynthesis and within the state assignment of Ministry of Science and Higher Education of the Russian Federation (theme No. 122032200240-8) in part of GB cells characterization and PGs expression.

Conflicts of interest

All authors declared that there are no conflicts of interest.

Ethical approval and consent to participate

The human glioma cell lines U87, U343, HS683, LN18, LN71, LN215, and LN405 used in this work were purchased from the American Tissue Culture Collection (ATCC, Manassas, VA, USA). Cell lines were accompanied by authentication test certificates and cultured according to the ATCC recommendations.

Consent for publication

The manuscript does not contain individual details, images or videos.

REFERENCES

1. Torrisi F, Alberghina C, D'Aprile S, et al. The hallmarks of glioblastoma: heterogeneity, intercellular crosstalk and molecular signature of invasiveness and progression. *Biomedicines* 2022;10:806. DOI PubMed PMC
2. Lauko A, Lo A, Ahluwalia MS, Lathia JD. Cancer cell heterogeneity & plasticity in glioblastoma and brain tumors. *Semin Cancer Biol* 2022;82:162-75. DOI PubMed PMC
3. Becker AP, Sells BE, Haque SJ, Chakravarti A. Tumor heterogeneity in glioblastomas: from light microscopy to molecular pathology. *Cancers* 2021;13:761. DOI PubMed PMC
4. Hutóczki G, Virga J, Birkó Z, Klekner A. Novel concepts of glioblastoma therapy concerning its heterogeneity. *Int J Mol Sci* 2021;22:10005. DOI PubMed PMC
5. Oliver L, Lalier L, Salaud C, Heymann D, Cartron PF, Vallette FM. Drug resistance in glioblastoma: are persisters the key to therapy? *Cancer Drug Resist* 2020;3:287-301. DOI PubMed PMC
6. Stupp R, Mason WP, van den Bent MJ, et al. Radiotherapy plus concomitant and adjuvant temozolomide for glioblastoma. *N Engl J Med* 2005;352:987-96. DOI PubMed
7. Tan AC, Ashley DM, López GY, Malinzak M, Friedman HS, Khasraw M. Management of glioblastoma: state of the art and future directions. *CA Cancer J Clin* 2020;70:299-312. DOI PubMed
8. Lee SY. Temozolomide resistance in glioblastoma multiforme. *Genes Dis* 2016;3:198-210. DOI PubMed PMC
9. Arora A, Somasundaram K. Glioblastoma vs temozolomide: can the red queen race be won? *Cancer Biol Ther* 2019;20:1083-90. DOI PubMed PMC
10. Zhang J, Stevens MF, Bradshaw TD. Temozolomide: mechanisms of action, repair and resistance. *Curr Mol Pharmacol* 2012;5:102-14. DOI PubMed
11. Tomar MS, Kumar A, Srivastava C, Shrivastava A. Elucidating the mechanisms of temozolomide resistance in gliomas and the strategies to overcome the resistance. *Biochim Biophys Acta Rev Cancer* 2021;1876:188616. DOI PubMed
12. Singh N, Miner A, Hennis L, Mittal S. Mechanisms of temozolomide resistance in glioblastoma - a comprehensive review. *Cancer Drug Resist* 2021;4:17-43. DOI PubMed PMC
13. Choo M, Mai VH, Kim HS, et al. Involvement of cell shape and lipid metabolism in glioblastoma resistance to temozolomide. *Acta Pharmacol Sin* 2023;44:670-9. DOI PubMed PMC
14. Kopecka J, Riganti C. Overcoming drug resistance in glioblastoma: new options in sight? *Cancer Drug Resist* 2021;4:512-6. DOI PubMed PMC
15. Bao Z, Wang Y, Wang Q, et al. Intratumor heterogeneity, microenvironment, and mechanisms of drug resistance in glioma recurrence and evolution. *Front Med* 2021;15:551-61. DOI
16. Virtuoso A, Giovannoni R, De Luca C, et al. The glioblastoma microenvironment: morphology, metabolism, and molecular signature of glial dynamics to discover metabolic rewiring sequence. *Int J Mol Sci* 2021;22:3301. DOI PubMed PMC
17. Dapash M, Hou D, Castro B, Lee-Chang C, Lesniak MS. The interplay between glioblastoma and its microenvironment. *Cells* 2021;10:2257. DOI PubMed PMC
18. DeCordova S, Shastri A, Tsolaki AG, et al. Molecular heterogeneity and immunosuppressive microenvironment in glioblastoma. *Front Immunol* 2020;11:1402. DOI PubMed PMC
19. Eisenbarth D, Wang YA. Insights into the co-evolution of glioblastoma and associated macrophages. *J Cancer Metastasis Treat* 2023;9:14. DOI
20. Seker-Polat F, Pinarbasi Degirmenci N, Solaroglu I, Bagci-Onder T. Tumor cell infiltration into the brain in glioblastoma: from mechanisms to clinical perspectives. *Cancers* 2022;14:443. DOI PubMed PMC
21. Marino S, Menna G, Di Bonaventura R, et al. The extracellular matrix in glioblastomas: a glance at its structural modifications in shaping the tumoral microenvironment-a systematic review. *Cancers* 2023;15:1879. DOI PubMed PMC
22. Towner RA, Zalles M, Saunders D, Smith N. Novel approaches to combat chemoresistance against glioblastomas. *Cancer Drug Resist* 2020;3:686-98. DOI PubMed PMC
23. Jiapaer S, Furuta T, Tanaka S, Kitabayashi T, Nakada M. Potential strategies overcoming the temozolomide resistance for glioblastoma. *Neurol Med Chir* 2018;58:405-21. DOI PubMed PMC
24. De Hauwer C, Camby I, Darro F, et al. Dynamic characterization of glioblastoma cell motility. *Biochem Biophys Res Commun* 1997;232:267-72. DOI
25. Hagemann C, Anacker J, Haas S, et al. Comparative expression pattern of matrix-metalloproteinases in human glioblastoma cell-lines and primary cultures. *BMC Res Notes* 2010;3:293. DOI PubMed PMC
26. Ishii N, Maier D, Merlo A, et al. Frequent co-alterations of TP53, p16/CDKN2A, p14ARF, PTEN tumor suppressor genes in human glioma cell lines. *Brain Pathol* 1999;9:469-79. DOI PubMed PMC
27. Bady P, Diserens AC, Castella V, et al. DNA fingerprinting of glioma cell lines and considerations on similarity measurements. *Neuro Oncol* 2012;14:701-11. DOI PubMed PMC
28. Studer A, de Tribolet N, Diserens AC, et al. Characterization of four human malignant glioma cell lines. *Acta Neuropathol* 1985;66:208-17. DOI
29. Guo M, van Vliet M, Zhao J, et al. Identification of functionally distinct and interacting cancer cell subpopulations from glioblastoma with intratumoral genetic heterogeneity. *Neurooncol Adv* 2020;2:vdaa061. DOI PubMed PMC
30. Al-Mayhani MT, Grenfell R, Narita M, et al. NG2 expression in glioblastoma identifies an actively proliferating population with an

aggressive molecular signature. *Neuro Oncol* 2011;13:830-45. DOI PubMed PMC

31. Innes JA, Lowe AS, Fonseca R, et al. Phenotyping clonal populations of glioma stem cell reveals a high degree of plasticity in response to changes of microenvironment. *Lab Invest* 2022;102:172-84. DOI PubMed PMC
32. Rehfeld M, Matschke J, Hagel C, Willenborg K, Glatzel M, Bernreuther C. Differential expression of stem cell markers in proliferating cells in glioma. *J Cancer Res Clin Oncol* 2021;147:2969-82. DOI PubMed PMC
33. Brown DV, Filiz G, Daniel PM, et al. Expression of CD133 and CD44 in glioblastoma stem cells correlates with cell proliferation, phenotype stability and intra-tumor heterogeneity. *PLoS One* 2017;12:e0172791. DOI PubMed PMC
34. Mooney KL, Choy W, Sidhu S, et al. The role of CD44 in glioblastoma multiforme. *J Clin Neurosci* 2016;34:1-5. DOI
35. Louis DN, Perry A, Wesseling P, et al. The 2021 WHO classification of tumors of the central nervous system: a summary. *Neuro Oncol* 2021;23:1231-51. DOI PubMed
36. Berger TR, Wen PY, Lang-Orsini M, Chukwueke UN. World Health Organization 2021 classification of central nervous system tumors and implications for therapy for adult-type gliomas: a review. *JAMA Oncol* 2022;8:1493-501. DOI PubMed
37. Kurokawa R, Kurokawa M, Baba A, et al. Major changes in 2021 World Health Organization classification of central nervous system tumors. *Radiographics* 2022;42:1474-93. DOI
38. Reuss DE. Updates on the WHO diagnosis of IDH-mutant glioma. *J Neurooncol* 2023;162:461-9. DOI PubMed PMC
39. Trifănescu OG, Trifănescu RA, Mitrică R, et al. Upstaging and downstaging in gliomas-clinical implications for the fifth edition of the World Health Organization classification of tumors of the central nervous system. *Diagnostics* 2023;13:197. DOI PubMed PMC
40. Lu Y, Shao Y. Multicellular biomarkers of drug resistance as promising targets for glioma precision medicine and predictors of patient survival. *Cancer Drug Resist* 2022;5:511-33. DOI PubMed PMC
41. Listik E, Toma L. Glypican-1 in human glioblastoma: implications in tumorigenesis and chemotherapy. *Oncotarget* 2020;11:828-45. DOI PubMed PMC
42. Kolliopoulos C, Ali MM, Castillejo-Lopez C, Heldin CH, Heldin P. CD44 depletion in glioblastoma cells suppresses growth and stemness and induces senescence. *Cancers* 2022;14:3747. DOI PubMed PMC
43. Gudbergsson JM, Christensen E, Kostrikov S, et al. Conventional treatment of glioblastoma reveals persistent $CD44^{+}$ subpopulations. *Mol Neurobiol* 2020;57:3943-55. DOI
44. Tran VM, Wade A, McKinney A, et al. Heparan sulfate glycosaminoglycans in glioblastoma promote tumor invasion. *Mol Cancer Res* 2017;15:1623-33. DOI PubMed PMC
45. Xiong A, Spyrou A, Forsberg-nilsson K. Involvement of heparan sulfate and heparanase in neural development and pathogenesis of brain tumors. In: Vlodavsky I, Sanderson RD, Ilan N, editors. Heparanase. Cham: Springer International Publishing; 2020. pp. 365-403. DOI
46. Jaime-Ramirez AC, Dmitrieva N, Yoo JY, et al. Humanized chondroitinase ABC sensitizes glioblastoma cells to temozolomide. *J Gene Med* 2017:19. DOI PubMed PMC
47. Tsidulko AY, Bezier C, de La Bourdonnaye G, et al. Conventional anti-glioblastoma chemotherapy affects proteoglycan composition of brain extracellular matrix in rat experimental model in vivo. *Front Pharmacol* 2018;9:1104. DOI PubMed PMC
48. Tsidulko AY, Shevelev OB, Khotskina AS, et al. Chemotherapy-induced degradation of glycosylated components of the brain extracellular matrix promotes glioblastoma relapse development in an animal model. *Front Oncol* 2021;11:713139. DOI PubMed PMC
49. Aladev SD, Sokolov DK, Strokotova AV, et al. Dexamethasone effects on the expression and content of glycosylated components of mouse brain tissue. *Adv Mol Onkol* 2023;10:25-39. (in Russian). DOI
50. Sokolov DK, Shevelev OB, Khotskina AS, et al. Dexamethasone inhibits heparan sulfate biosynthetic system and decreases heparan sulfate content in orthotopic glioblastoma tumors in mice. *Int J Mol Sci* 2023;24:10243. DOI PubMed PMC